

Figure S1 (a) The mechanical behavior of the interface friction  $f$ .<sup>1</sup> (b) Generation process of beads ( $N=4$ ).

Gupta et. al systematically study the different interface friction cases and proposed a new coarse-grained CNT model which could precisely simulate different friction load between CNTs by tuning parameter  $f$ .<sup>1</sup> In order to clarify the meaning of  $f$ , we redraw the mechanical behavior of the interface friction as shown in Figure S1a. When the friction exists between two tubes, take a fixed bead and a tube that moves parallel to it for analysis. It can be seen that the fixed bead and beads  $z_2, z_3$  are touching, and there are the normal force  $F_n$  and tangential force  $F_t$  between two beads. However, distinct

from the macroscopic friction, there is no direct correlation between the interface friction and the normal force. It is because that buckled cross-section induced by pressure may cause the crosslinks loose, rather than producing normal force. The tangential force  $F_t$  is expressed as a linear function, as shown in Figure S1a and interfacial friction is described in <sup>1</sup>

$$f = \frac{-2k_t a^2}{r_0^2} [\ln(\phi + \sqrt{\phi^2 - 1})]^2$$

Where,  $\phi=D/a$  is the factor about bead diameter and inter-tube distance,  $D$  is the diameter of bead,  $a$  is the distance between two tubes,  $k_t$  is tangential stiffness for interactions,  $r_0$  is the equilibrium length. Thus, the value of interface friction is related on  $D$ ,  $a$ ,  $k_t$ ,  $r_0$ . The unit of  $f$  is nN/ Å, which means the friction force per length.

Figure S1b depicts the generation process of beads when  $N=4$ . At the beginning, when the index of bead is less than 4, the angle of next generated bead is same as the previous one and these beads are in a straight line. If the number of beads reaches  $N=4$ , the new bead is randomly generated in the specific region where the angle  $\theta_1$  is in the range of  $-\pi/6$  and  $\pi/6$  as shown in Figure S1b. However, due to the non-periodic boundary of the film, there inevitably exists the situation that newly generated position exceeds the boundary of the box which could be called as “boundary effect” in this work. Thus, to ensure the integrity of the model, the angle  $\theta_3$  is in the range of  $-\pi/2$  and  $\pi/2$  to make sure that newly-generated bead is inside box. Accordingly, it can be inferred that  $N$  affects the entanglement degree of film, that is, when  $N$  is small, the deflection frequency of bead increases and the entanglement of the film is high which could also be seen from the relationship between bending energy of the film and

parameter  $N$  in Figure 3b. It is worth noting that, in order to systematically investigate the influence of parameter  $N$  on the mechanical properties of the film, the length and width of box are set as  $1000 \text{ \AA} * 1000 \text{ \AA}$ . Therefore, when  $N$  is big, the probability of “boundary effect” is high. From the analytical results in this work, when  $N$  is greater than 500 (length of CNT segment is longer than half the size of the box), the effect of “boundary effect” on the mechanical properties of the buckypaper gets severe.

Table S1 Parameters for the coarse-grained model of (5,5) SWCNT<sup>1</sup>

$r_0$	$k_r$	$k_\theta$	$\varepsilon$	$\sigma$
(Å)	(kcal/mol Å <sup>2</sup> )	(kcal/mol rad <sup>2</sup> )	(kcal/mol)	(Å)
2	2500	35750	9.323	0.4205

Where  $r_0$  is the equilibrium length,  $k_r$  is the stretching constant,  $k_\theta$  is the bending constant,  $\varepsilon$  is the depth of the potential well,  $\sigma$  is the equilibrium distance where the inter-bead potential is zero.

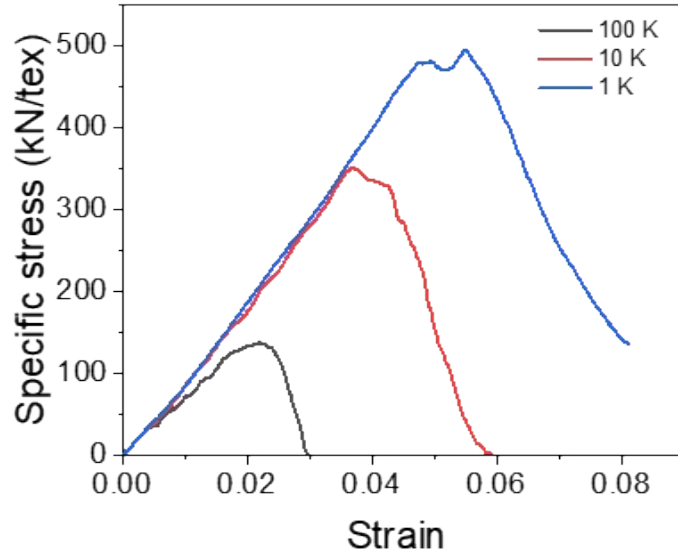


Figure S2 Specific stress-strain curves of SWBP ( $N=1000, f=100$ ) under different temperature

In order to explore the mechanical properties of buckypaper under different temperature, the SWBP ( $N=1000, f=100$ ) is stretched under different temperature (1 K, 10 K, 100 K) and corresponding stress-strain curves are shown in Figure S2. It can be seen that with the increasing of temperature, the mechanical behaviors and specific stress-strain curves are similar under different temperatures. Due to the increase in temperature, CNT fluctuates violently, leading to premature fracture and a decrease in strength. Besides, the films under different temperatures hold the nearly same Young's modulus, thus, the influence of temperature on the Young's modulus is negligible.

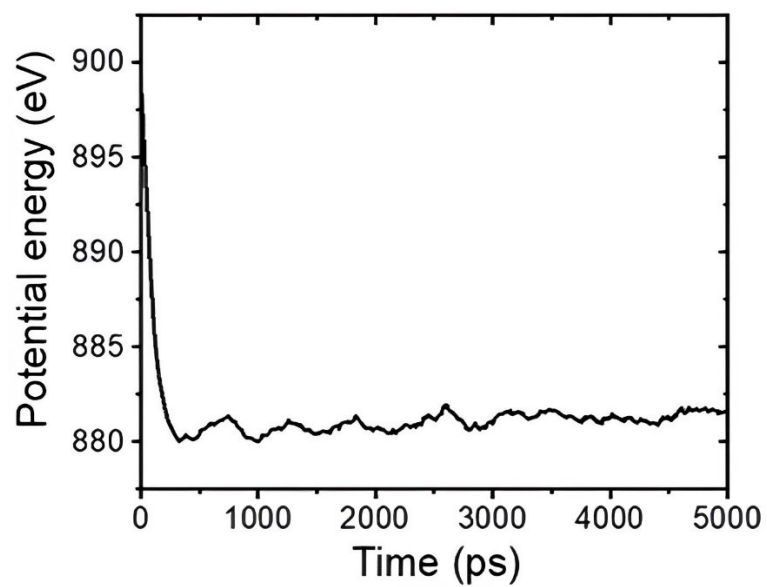


Figure S3 Potential energy of representative BP ( $N=300, f=0$ ) during the relaxation process.

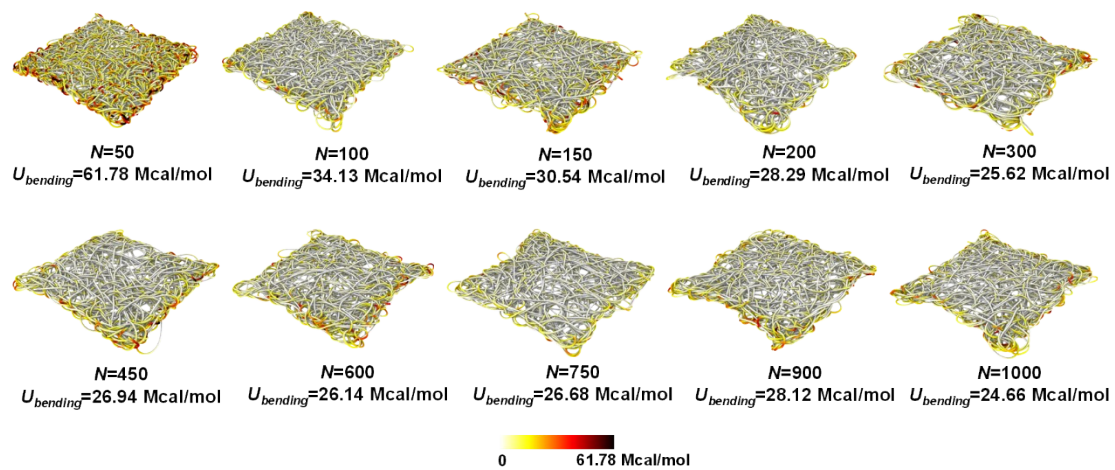


Figure S4 SWBP models of different  $N$  ( $f=0$ ), atoms are colored by bending energy.

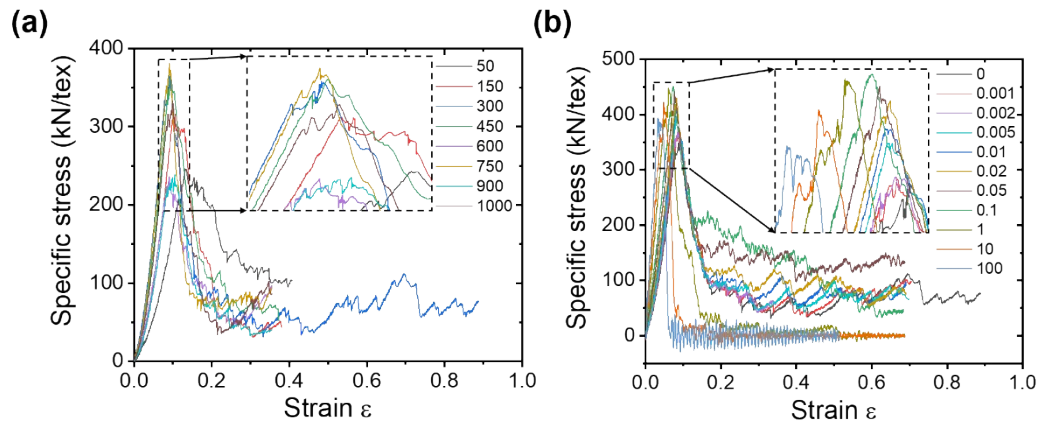


Figure S5 (a) The specific stress-strain curves of SWBPs with different  $N$  ( $f=0$ ). (b) The specific stress-strain curves of SWBPs with different  $f$  ( $N=300$ ).

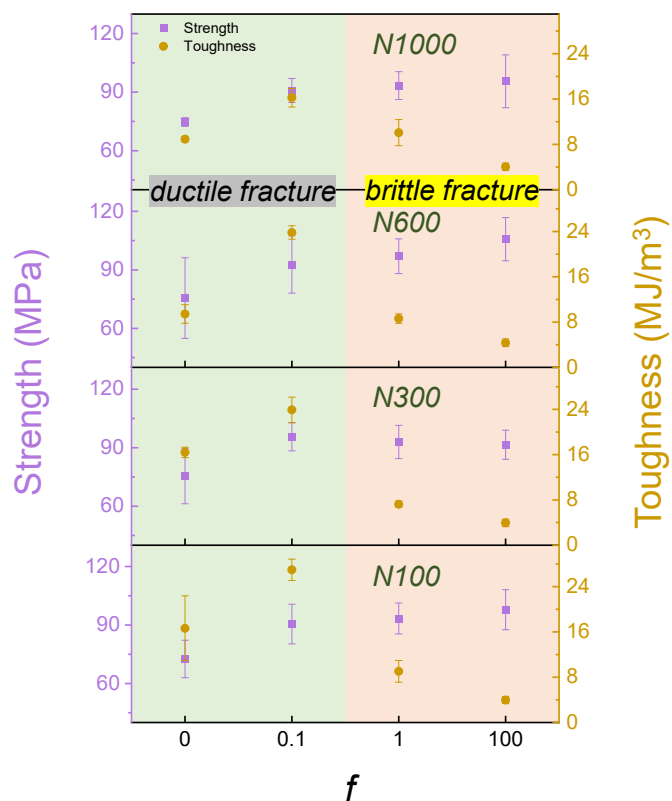


Figure S6 The strength and toughness of different initial SWBPs

The mechanical properties of CNT buckypaper with  $N$  ( $N=100, 300, 600, 1000$ ) and  $f$  ( $f=0, 0.1, 1, 100$ ) are investigated and the corresponding strength and toughness are shown in Figure S6. The toughness represents the area closed by the stress-strain curve. From Figure S6, it can be seen that with the increasing of  $f$ , the strength of SWBP shows an upward trend generally, regardless of  $N$ . On the other hand, as  $f$  increases, the toughness of SWBP enhances first and then decreases, which mainly due to the ductile-brittle transition. The results show that when  $f$  is higher than 1, the brittle fracture occurs at a lower strain, leading to a sharp decline in toughness.

## References:

1. N. Gupta, J. M. Alred, E. S. Penev and B. I. Yakobson, *Acs Nano*, 2021, **15**, 1342-1350.